

Lawrence Berkeley National Laboratory

Lawrence Berkeley National Laboratory

Title

Recent Developments and Applications of the Beam Simulation Code WARP

Permalink

<https://escholarship.org/uc/item/2j32b65x>

Author

Vay, J.-L.

Publication Date

2012-07-31

RECENT DEVELOPMENTS AND APPLICATIONS OF THE BEAM SIMULATION CODE WARP*

J.-L. Vay, P. A. Seidl[†], LBNL, USA
D. P. Grote, A. Friedman LLNL, USA

INTRODUCTION

The Particle-In-Cell (PIC) Framework Warp [1] was originally developed to simulate space-charge-dominated beam dynamics in induction accelerators for heavy-ion fusion (HIF). It is currently being developed primarily by the Heavy Ion Fusion Science Virtual National Laboratory (HIFS-VNL) collaboration, to guide the development of accelerators that can deliver beams suitable for high energy density experiments [2] and implosion of inertial fusion capsules [3]. In recent years, the physics models in the code have been generalized, so that Warp can model beam injection, complicated boundary conditions, denser plasmas, a wide variety of accelerator lattice components, the non-ideal physics of beams interacting with walls and plasmas, as well as laser-plasma interactions.

The user interface of Warp is Python, a high level, object oriented, interactive and scripting language designed for ease of use and flexibility. The interface between the Fortran and Python is created by the Forthon package [4]. This code architecture enables rapid prototyping and great versatility, and allows users to write their own extensions. Warp has recently been augmented with various novel methods including PIC with adaptive mesh refinement [5], a large-timestep mover for particles of arbitrary magnetized species [6, 7], a new relativistic Lorentz invariant leapfrog particle pusher [8], simulations in Lorentz boosted frames [9, 10], an electromagnetic solver with tunable numerical dispersion and efficient stride-based digital filtering [11]. With its new capabilities and thanks to a design that allows for a high degree of versatility, the range of application of Warp has considerably widened far beyond the initial application to the Heavy Ion Fusion Science program.

The code now has an international user base and is being applied to projects both within and far removed from the HIF community. Ongoing or recent examples of applications outside HIF include the modeling of plasma traps for the production of anti-Hydrogen [12], Paul traps [13, 14], non-conventional Penning-Malmberg micro-trap [15], transport of electron beams in the UMER ring [16], ECR ion sources [17], capture and control of laser-accelerated proton beams [18], and fundamental studies of multipacting [19]. It is also applied to the study and design of existing and next generation high-energy accelerators including the study of electron cloud effects [20], coherent

synchrotron radiation [21] and laser wakefield acceleration [10].

We concentrate below on the description of new diagnostics for computing the local energy spread (and temperature) that properly accounts for linear correlations that arise from the discrete binning along each physical dimension. The new diagnostic is an extension of the one developed in the code BPIC [22] and described in [23] (a related procedure is also described in [24]). We also describe further extension.

CALCULATION OF THE TEMPERATURE AND ENERGY SPREAD IN WARP

Assuming a distribution of particles $f(X, V)$ of positions $X = \{x, y, z\}$ and velocities $V = \{v_x, v_y, v_z\}$, the temperature kT_u along the direction $u = x, y$ or z and the kinetic energy spread δK at $X_0 = \{x_0, y_0, z_0\}$ are defined as being directly related respectively to the variance of the velocity components and the standard deviation of the kinetic energy as:

$$kT_u = \frac{1}{2} m \overline{(v_u - \bar{v}_u)^2}, \quad (1)$$

$$= \frac{1}{2} m \frac{\int_{-\infty}^{\infty} f(X_0, v_u) (v_u - \bar{v}_u)^2 \cdot dv_u}{\int_{-\infty}^{\infty} f(X_0, v_u) \cdot dv_u}, \quad (2)$$

$$\delta K = \sqrt{\overline{(K - \bar{K})^2}}, \quad (3)$$

$$= \frac{1}{2} m \sqrt{\frac{\int_0^{\infty} f(X_0, V) (K - \bar{K})^2 \cdot dK}{\int_0^{\infty} f(X_0, V) \cdot dK}}, \quad (4)$$

where $m, v = \sqrt{v_x^2 + v_y^2 + v_z^2}$ and $K = \frac{1}{2} m v^2$ are respectively the mass, velocity and kinetic energy of the particles. The mean values of the velocity components and kinetic energy are given by

$$\bar{v}_u = \frac{\int_{-\infty}^{\infty} f(X_0, v_u) v_u \cdot dv_u}{\int_{-\infty}^{\infty} f(X_0, v_u) \cdot dv_u}, \quad (5)$$

$$\bar{K} = \frac{\int_0^{\infty} f(X_0, V) K \cdot dK}{\int_0^{\infty} f(X_0, V) \cdot dK}. \quad (6)$$

The above definitions apply to infinitesimal volumes and continuous density functions f and can be interpreted as the mathematical limit of discretized equivalent definitions for a finite size sample of N particles and finite volumes $\delta\Omega$ when $N \rightarrow \infty$ and $\delta\Omega \rightarrow 0$. At these limits, correlations between velocity (or kinetic energy) with position vanish and do not need to appear explicitly in the calculation of

* Supported by the US-DOE under Contracts DE-AC02-05CH1123 and DE-AC52-07NA27344, and the SciDAC/ComPASS project. Used resources of the National Energy Research Supercomputer Center (NERSC).

[†] jlway@lbl.gov

temperature or energy spread. In practice, however, both N and $\delta\Omega$ are finite, and correlations need eventually to be accounted for.

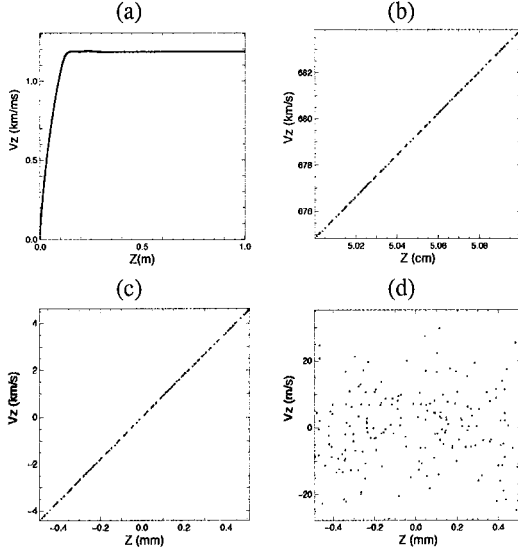


Figure 1: Longitudinal $z - v_z$ phase-space projection from a simulation of NDCX-I for (a) $0 < z < 1$ m, (b) a 1 mm long sample between $6.4 \text{ mm} < r < 7.7 \text{ mm}$ and $5 \text{ cm} < z < 5.1 \text{ cm}$, (c) same sample as (b) with averages removed along z and v_z , (d) same sample as (c) with linear correlation between v_z and z removed.

As an example, we consider a snapshot from a simulation of NDCX-I [25]. The longitudinal phase space $z - v_z$ is plotted in Fig. 1-(a) for $0 < z < 1$ m, while a 1 mm long sample for $5 \text{ cm} < z < 5.1 \text{ cm}$ and $6.4 \text{ mm} < r < 7.7 \text{ mm}$ is shown in Fig. 1-(b), and with averages removed in Fig. 1-(c). A linear correlation is clearly visible, which would give rise to an overestimate of the local temperature if not removed. The sample with linear correlation removed is shown in Fig. 1-(d). Note the change of scales.

Removing the linear correlations necessitates the knowledge of the correlation coefficients for each spatial direction, which are computed as follows.

Let us assume that at $X_0 = \{x_0, y_0, z_0\}$, the kinetic energy $K_1 = K - \bar{K}$ has a linear correlation with the sample positions x, y and z , such that $K_1 = K_2 + a_1X + b_1Y + c_1Z$ where $X = x - \bar{x}$, $Y = y - \bar{y}$, $Z = z - \bar{z}$, $\overline{XK_2} = \overline{YK_2} = \overline{ZK_2} = 0$, and a_1, b_1 and c_1 are scalars giving the "slopes" of the coupling in each spatial direction. From the definitions given above, one can write

$$\overline{XK_2} = \overline{X(K_1 - a_1X - b_1Y - c_1Z)} = 0, \quad (7)$$

$$\overline{YK_2} = \overline{Y(K_1 - a_1X - b_1Y - c_1Z)} = 0 \quad (8)$$

$$\overline{ZK_2} = \overline{Z(K_1 - a_1X - b_1Y - c_1Z)} = 0 \quad (9)$$

such that a_1, b_1 and c_1 are the solutions of the linear system

$$\begin{cases} \overline{X^2}a_1 + \overline{XY}b_1 + \overline{XZ}c_1 - \overline{XK_1} = 0 \\ \overline{YX}a_1 + \overline{Y^2}b_1 + \overline{YZ}c_1 - \overline{YK_1} = 0 \\ \overline{ZX}a_1 + \overline{ZY}b_1 + \overline{Z^2}c_1 - \overline{ZK_1} = 0 \end{cases} \quad (10)$$

The system is solved explicitly in Warp. The same procedure is used to remove linear correlations between v_x, v_y and v_z for the temperature calculations.

The new diagnostic has been applied to the analysis of the evolution of velocity spread and longitudinal cooling in the NDCX-I accelerator (see [26], Fig. 3), establishing that there is no significant broadening of the energy distribution due to intrinsic mechanisms such as translaminar effects or transverse-longitudinal anisotropy instability.

Although not present (or discernable) in the 1 mm sample that was shown, higher order correlations can be present, as shown in Fig. 2 for a 4 mm long sample, and should ideally be removed. In the present version of the Warp diagnostic, only the linear correlation is removed, as a compromise between accuracy and speed. In the future, the subroutine could be modified to recursively remove spatial correlations up-to an arbitrary order, as described below.

More generally, one can write the kinetic energy distribution as the weighted sum of powers of X, Y and Z up to order n

$$K = K_{n+1} + \sum_{i=0}^n (a_i X^i + b_i Y^i + c_i Z^i + d_i) \quad (11)$$

while imposing $\overline{X^n K_{n+1}} = \overline{X^n K_{n+1}} = \overline{X^n K_{n+1}} = 0$ and $\overline{K_n} = 0$. The distribution K_{n+1} can be computed recursively using

$$K_{n+1} = K_n - a_n X^n - b_n Y^n - c_n Z^n - d_n \quad (12)$$

and solving for

$$\begin{cases} \overline{X^{2n}a_n} + \overline{X^n Y^n b_n} + \overline{X^n Z^n c_n} + \overline{X^n d_n} = \overline{X^n K_n} \\ \overline{Y^n X^n a_n} + \overline{Y^{2n}b_n} + \overline{Y^n Z^n c_n} + \overline{Y^n d_n} = \overline{Y^n K_n} \\ \overline{Z^n X^n a_n} + \overline{Z^n Y^n b_n} + \overline{Z^{2n}c_n} + \overline{Z^n d_n} = \overline{Z^n K_n} \\ \overline{X^n a_n} + \overline{Y^n b_n} + \overline{Z^n c_n} + d_n = 0 \end{cases} \quad (13)$$

We note that for n odd, then $\overline{X^n} = \overline{Y^n} = \overline{Z^n} = 0$, giving $d_n = 0$ and the system to solve simplifies to

$$\begin{cases} \overline{X^{2n}a_n} + \overline{X^n Y^n b_n} + \overline{X^n Z^n c_n} = \overline{X^n K_n} \\ \overline{Y^n X^n a_n} + \overline{Y^{2n}b_n} + \overline{Y^n Z^n c_n} = \overline{Y^n K_n} \\ \overline{Z^n X^n a_n} + \overline{Z^n Y^n b_n} + \overline{Z^{2n}c_n} = \overline{Z^n K_n} \end{cases} \quad (14)$$

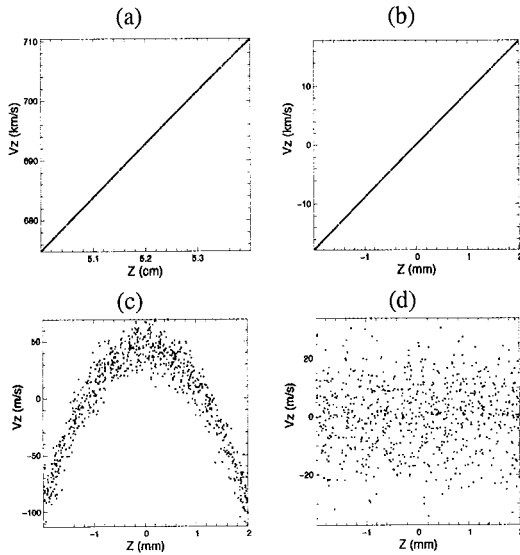


Figure 2: Longitudinal $z - v_z$ phase-space projection from a simulation of NDCX-I for (a) a 4 mm long sample between $6.4 \text{ mm} < r < 7.7 \text{ mm}$ and $5 \text{ cm} < z < 5.4 \text{ cm}$, (b) same sample as (a) with averages removed along z and v_z , (c) same sample as (b) with linear correlation between v_z and z removed (d) same sample as (c) with quadratic correlation between v_z and z removed.

The recursive procedure that was just described has been applied successfully to the sample case shown in Fig. 2, for removing the quadratic correlation between v_z and z that is visible in Fig. 2-(c), giving the uncorrelated distribution plotted in Fig. 2-(d). Comparing Fig. 1-(d) and 2-(d) shows that removing higher order correlations allows for larger samples, reducing the size of the diagnostic arrays and improving the statistics per cell. This procedure will be implemented in the future, adding the option of either setting a maximum level of recursion level (or equivalently highest order of correlation to be removed) or setting a tolerance for stopping the recursion on the difference between the temperature (or energy spread) value at two consecutive recursion levels. Sorting the macroparticle data spatially by grid cells beforehand would allow for each cell to reach independent levels of recursion.

REFERENCES

- [1] D. Grote, A. Friedman, J.-L. Vay, I. Haber, AIP Conference Proceedings 749 (2005) 55–8.
- [2] A. Friedman, J. Barnard, R. Cohen, D. Grote, S. Lund, W. Sharp, A. Faltens, E. Henestroza, J.-Y. Jung, J. Kwan, E. Lee, M. Leitner, B. Logan, J.-L. Vay, W. Waldron, R. Davidson, M. Dorf, E. Gilson, I. Kaganovich, Phys. Plasmas 17 (5) (2010) 056704.
- [3] B. Logan, F. Bieniosek, C. Celata, J. Coleman, W. Greenway, E. Henestroza, J. Kwan, E. Lee, M. Leitner, P. Roy, P. Seidl, J.-L. Vay, W. Waldron, S. Yu, J. Barnard, R. Cohen, A. Friedman, D. Grote, M. K. Covo, A. Molvik, S. Lund, W. Meier, W. Sharp, R. Davidson, P. Efthimion, E. Gilson, L. Grisham, I. Kaganovich, H. Qin, A. Sefkow, E. Startsev, D. Welch, C. Olson, Nucl. Instr. and Methods A 577 (2007) 1–7.
- [4] [Http://hifweb.lbl.gov/Forthon](http://hifweb.lbl.gov/Forthon).
- [5] J.-L. Vay, P. Colella, J. Kwan, P. McCorquodale, D. Serafini, A. Friedman, D. Grote, G. Westenskow, J.-C. Adam, A. Heron, I. Haber, Phys. Plasmas 11 (5) (2004) 2928–2934.
- [6] R. Cohen, A. Friedman, M. Covo, S. Lund, A. Molvik, F. Bieniosek, P. Seidl, J. Vay, P. Stoltz, S. Veitzer, Phys. Plasmas 12 (5) (2005) 056708.
- [7] R. H. Cohen, A. Friedman, D. P. Grote, J. L. Vay, Nucl. Instr. and Methods A 606 (1-2) (2009) 53–55.
- [8] J. L. Vay, Phys. Plasmas 15 (5) (2008) 056701.
- [9] J.-L. Vay, Phys. Rev. Lett. 98 (13) (2007) 130405/1–4.
- [10] J. L. Vay, C. G. R. Geddes, E. Esarey, C. B. Schroeder, W. P. Leemans, E. Cormier-Michel, D. P. Grote, Phys. Plasmas 18 (12) (2011) 123103.
- [11] J. L. Vay, C. G. R. Geddes, E. Cormier-Michel, D. P. Grote, J. Comput. Phys. 230 (15) (2011) 5908–5929.
- [12] K. Gomberoff, J. Fajans, A. Friedman, D. Grote, J.-L. Vay, J. S. Wurtele, Phys. Plasmas 14 (10) (2007).
- [13] E. P. Gilson, R. C. Davidson, M. Dorf, P. C. Efthimion, R. Majeski, M. Chung, M. S. Gutierrez, A. N. Kabcenell, Phys. Plasmas 17 (5) (2010).
- [14] S. Ohtsubo, M. Fujioka, H. Higaki, K. Ito, H. Okamoto, H. Sugimoto, S. M. Lund, Phys. Rev. ST-AB 13 (4) (2010).
- [15] P. Folegati, J. Xu, M. H. Weber, K. G. Lynn, J. of Physics: Conference Series 262 (1) (2011) 012021.
- [16] I. Haber, S. Bernal, B. Beaudoin, A. Cornacchia, D. Feldman, R. B. Feldman, R. Fiorito, K. Fiuza, T. F. Godlove, R. A. Kishek, P. G. O’Shea, B. Quinn, C. Papadopoulos, M. Reiser, D. Stratakis, D. Sutter, J. C. T. Thangaraj, K. Tian, M. Walter, C. Wu, Nucl. Instr. and Methods A 606 (1-2) (2009) 64–68.
- [17] D. Winklehner, D. Todd, J. Benitez, M. Strohmeier, D. Grote, D. Leitner, J. Instrumentation 5 (2010).
- [18] F. Nürnberg, A. Friedman, D. P. Grote, K. Harres, B. G. Logan, M. Schollmeier, M. Roth, J. of Physics: Conference Series 244 (2) (2010) 022052.
- [19] R. A. Kishek, Phys. Rev. Lett. 108 (2012) 035003.
- [20] J.-L. Vay, M. A. Furman, M. Venturini, Proc. Particle Accelerator Conference, New-York, NY, USA, 2011, WEP154.
- [21] W. Fawley, J.-L. Vay, Proc. IPAC 2010, paper TUPEC064, Kyoto, Japan, 2010.
- [22] J.-L. Vay and C. Deutsch, Phys. Plasmas 5 (1998) 1190.
- [23] J.-L. Vay, Ph.D. thesis, Orsay, France, 1996
- [24] E. Cormier-Michel, B. A. Shadwick, C. G. R. Geddes, E. Esarey, C. B. Schroeder, and W. P. Leemans, Phys. Rev. E 78 (2008) 016404.
- [25] P.A. Seidl et al., Proc. XXIV Linear Accelerator Conf. LINAC’08, Victoria, BC, Canada (2008) TH203.
- [26] I. D. Kaganovich, S. Massidda, E. A. Startsev, R. C. Davidson, J.-L. Vay, A. Friedman, Nucl. Instr. and Methods A 678 (2012) 48–63.

This document was prepared as an account of work sponsored by the United States Government. While this document is believed to contain correct information, neither the United States Government nor any agency thereof, nor The Regents of the University of California, nor any of their employees, makes any warranty, express or implied, or assumes any legal responsibility for the accuracy, completeness, or usefulness of any information, apparatus, product, or process disclosed, or represents that its use would not infringe privately owned rights. Reference herein to any specific commercial product, process, or service by its trade name, trademark, manufacturer, or otherwise, does not necessarily constitute or imply its endorsement, recommendation, or favoring by the United States Government or any agency thereof, or The Regents of the University of California. The views and opinions of authors expressed herein do not necessarily state or reflect those of the United States Government or any agency thereof or The Regents of the University of California.

This work was supported by the Director, Office of Science, Office of Fusion Energy Sciences, of the U.S. Department of Energy under Contract No. DE-AC02-05CH11231.